Binding Characteristics between Poly(ethylene glycol) and Hydrophilic Modified Ibuprofen in Aqueous Solution

Duo Wei, Lingling Ge, and Rong Guo*

School of Chemistry and Chemical Engineering, Yangzhou University, Yangzhou, People's Republic of China

Received: October 28, 2009; Revised Manuscript Received: February 4, 2010

The solubility of ibuprofen, a nonsteroidal anti-inflammatory drug (NSAID), is enhanced by synthesizing ibuprofen ester with a water-soluble polymer, poly(ethylene glycol) (PEG), and the product obtained functions as a nonionic surfactant (IBF-PEG800, IP800). The morphology and aggregation behavior of IP800 micelles and IP800/PEG complexes in aqueous solution are investigated by ^{1}H NMR technology, dynamic light scattering (DLS), isothermal titration calorimetry (ITC), and fluorescence resonance energy transfer (FRET). The microstructure of IP800 micelles is strongly related to the concentration of IP800. IP800 monomers can form looser micelles at relatively low concentrations and much tighter micelles at high concentrations. And the binding model of PEG with looser IP800 micelles dramatically depends on the molecular weight and concentration of PEG: PEG with lower molecular weight (MW $\leq$ 2000 Da) inserts to the interface of the hydrophilic corona and hydrophobic core of IP800 micelles; PEG with higher molecular weight (MW $>$ 2000 Da) binds to the surface of IP800 micelles, and one long PEG chain (6000 $<$ MW $\leq$ 20000 Da) wraps several IP800 micelles. Besides, the ratio of short chain PEG400 to IP800 micelles of the IP800/PEG complex is about 15:1 at a fixed concentration of IP800 (0.05 mM), and for the long chain PEG20000 it is 1:3−1:4.

1. Introduction

Ibuprofen, a nonsteroidal anti-inflammatory drug (NSAID), is widely used, because it produces fewer gastrointestinal adverse events.[1–3] However, the solubility of ibuprofen in water is poor, which affects pharmaceutical product development in nearly all therapeutic areas. At present, several methods are used to solve this problem.[4–6] A suspending liquid is made, and some stuffing is added to achieve slow release formulation in clinical practice; for example, a water-soluble polymer, poly(ethylene glycol) (PEG), is always used as a stabilizer in pharmaceuticals as a medicated premix.[7,8] And some research focuses on utilizing the hydrophobic core of surfactant aggregates to solubilize ibuprofen.[4,9] Nonionic surfactants, for example, polyoxyethylated surfactants, are the major type of surface active agents used in delivery systems since they are generally less toxic, less hemolytic, and less irritating to the afflicted part and tend to maintain physiological pH values in solution.

However, whatever the types of surfactants used in pharmaceuticals are, they have hydrophobic segments which will compete with ibuprofen to interact with COX and hence affect the virtue of ibuprofen. Since PEG can interact with ibuprofen by the hydrogen bond between the terminal hydroxyl of PEG and the carboxyl group of ibuprofen, we use PEG as a hydrophilic agent to modify ibuprofen and thus to improve its solubility and to prevent side effect as mentioned above[10] in this investigation. As we know, the carboxyl of ibuprofen has no effect on the virtue of this drug,[6,11,12] so the hydrophilic modified ibuprofen is safe to be used, which will be further investigated. Moreover, the product obtained, ibuprofen-PEG (IP800) has mutual solubility with water and is a polyoxyethylated nonionic surfactant, which will form organized molecular assembilies in aqueous solutions spontaneously and solubilize other hydrophobic drugs to display a synergy effect.

In surfactant systems, the interaction between water-soluble polymers and surfactants has received enormous attention, because the addition of polymer to the surfactant system would improve the properties, such as stability, dispersity, rheology.[13–18] For example, the interaction of poly(ethylene glycol) (PEG or PEO) with ionic surfactants such as sodium dodecyl sulfate (SDS), cesium perfluorooctanoate (CsPFO), and lithium perfluoronctanoate (LiPFO) has been investigated.[14,19–21] And the results indicate that the addition of PEG induces the surfactants to aggregate, and that the structure of the surface/PEG complexes depends on the concentration and molecular weight of PEG and on the hydrophobic segments of surfactants. Much research also proves that nonionic surfactants can interact with neutral polymer and form new aggregates.[16–18] However, the interaction of PEO/nonionic surfactants does not involve the same type of specificity in the binding of surfactant micelles to the polymer chain as that of PEO/ionic surfactants: nonionic surfactants have the same value for the critical micelle concentration (cmc) in the presence of the polymer as in water, in contrast to the considerably lower critical aggregation concentration (cac) when ionic surfactants interact with uncharged polymer.[22] Our group investigated the interaction between nonionic surfactant, Triton 100, and PEG;[23] the results indicate that the configuration of the PEG/Triton-100 complexes strongly depends on the molecular weight of PEG (MW_{PEG}), and the critical MW_{PEG} is 2000.

Based on the information about the interaction between PEG and surfactants investigated previously, the aim of this investigation is to check whether the characteristic behavior displayed by PEG/IP800 complexes with different MW_{PEG}s is peculiar or not and to get the information on the effect of PEG addition on the morphology and microstructure of hydrophilic modified ibuprofen (IP800) micelles in aqueous system, so as to optimize its application in pharmaceuticals. Hence, we chose DLS (dynamic light scattering), isothermal titration calorimetry (ITC),

* To whom correspondence should be addressed. E-mail: guorong@yzu.edu.cn. Fax: (+86) 514-87311374.

10.1021/jp910315e
Published on Web 02/23/2010

and ^{1}H NMR[14,24,25] to probe the changes of conformation and binding patterns in the mixture of IP800 and PEG in aqueous solution.

2. Experimental Section

2.1. Materials. ***2.1.1. Synthesis of Ibuprofen−Poly(ethylene glycol).*** PEG800 (0.15 mol), ibuprofen (0.1 mol) and toluene (20 mL) were mixed entirely and polymerized with 2−3 drops H_2SO_4 (>98%) as catalyst. The reaction solution was stirred at 120 °C for 6 h, and then cooled to room temperature, and adjusted pH to 7 by adding NaOH to yield water-soluble polyester. The solvent was evaporated at reduced pressure. This raw product was dissolved in diethyl ether at 0 °C. The undissolved impurity was separated by filtration, and then the diethyl ether was removed from the filtrate with a rotary evaporator. Finally, the raw product was purified by chromatographic separation. Standard methods were employed to determine the structure and purity of the product. (Figure S1 in the Supporting Information).

The investigated PEGs (MW_{PEG} = 400, 800, 1000, 2000, 4000, 6000, 10000, 20000) were Sigma-Aldrich Corp. products, and the distribution of MW agreed with a narrow Poisson distribution. Pyrene (>99%), 1-anilinonaphthalene-8-sulfornate (ANS) (99%), and 2-dimethyl-2-silapentare-5-sulfonate sodium (DSS, >97%) were also obtained from Sigma-Aldrich. Doubly distilled water was used for all the experiments.

2.2. Methods. ***2.2.1. Fluorescence Spectroscopy.*** Steady-state fluorescence experiments were performed on a RF-5301 luminescence spectrometer (Japan Shimadzu Company) equipped with a thermostatted water-circulating bath during the experiments. Solutions were equilibrated for at least 12 h before measurement. IP800 was the energy donor, ANS was the energy acceptor, and the excitation wavelength was set at 260 nm. The emission spectra were collected from 270 to 350 nm, and the excitation and emission slits were both fixed at 3.8 nm. The ANS concentration was 1.0×10^{-5} M.

The ratio of the fluorescence intensity of the first (371 nm, I_1) to the third (382 nm, I_3) vibration bands of pyrene was used to probe the polarity of the microenvironment around pyrene.[26,27] The emission spectra were measured in the wavelength range 350−500 with the excitation wavelength being 338 nm; the excitation and emission slits were both 3.0 nm. The pyrene concentration was 1.0×10^{-6} M.

2.2.2. Determination of T_c (Clouding Temperature). To determine T_c, a series of IP800 solutions were prepared at ambient temperature. These solutions were placed in a thermal bath, which was slowly heated until clouding was observed visually. The relative values of T_c are estimated to be reproducible to ±0.2 °C.

2.2.3. Dynamic Light Scattering. Measurements were carried out at a scattering angle 90° using an ALV 5022 laser light scattering (LLS) instrument (ALV Co., Gemany) equipped with a cylindrical He−Ne laser (model 1145 p-3083, output power = 22 mW at λ = 632.8 nm) in combination with an ALV sp-86 digital correlater with a sampling time range of 25 ns to 40 ms. The LLS cell was held in a thermostat index matching vat filled with purified dust-free toluene. All solutions were filtered through a Millipore filter with 0.8 or 1.2 μm pore size and thermostatted at 25 ± 0.1 °C for at least 12 h. Experiment duration was 10 min. Experiments were repeated twice or more times.

2.2.4. Surface Tension Measurement. Isothermal surface tension measurements were carried out by the pendant drop method using an optical contact angle measuring device (OCA40, Dataphysics, Germany). Every sample was measured twice or more times. Before approaching the experimental results themselves and their subsequent analysis, our account starts with the details of the experimental procedure to determine the equilibrium surface tension.[15] The surface tension γ obtained after 10 min equilibrium was used.

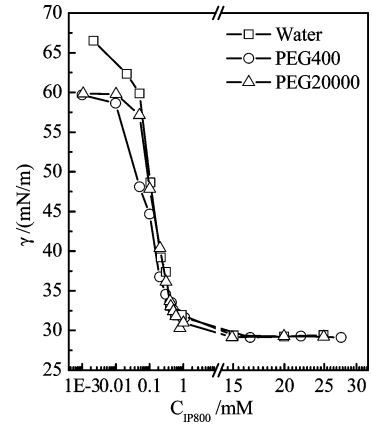

Figure 1. Surface tension as a function of IP800 concentration in the absence (□) and presence of 5.00 wt % PEG with MW_{PEG} = 400 (○) and 20 000 (△).

2.2.5. Isothermal Titration Microcalorimetry. ITC measurements were performed using a VP-ITC titration microcalorimeter from MicroCal Inc. (Northampton, MA) at (25 ± 0.1) kJ/mol[1]. A removable integrated injection-stirrer (250 μL) was filled with the desired concentration of IP800 aqueous solution, and it was titrated into the calorimeter vessel that initially was filled with water in portions of 3 μL at the constant stirring speed of 502 rpm to ensure thorough mixing. The duration of each injection was 10 s, and the time delay between successive injections was 240 s to allow equilibration. The reference cell was filled with double distilled water. Raw data were obtained as a plot of heating rate (μcal/s) against time (min). These raw data were then integrated to obtain a plot of observed enthalpy change per mole of injected IP800 (ΔH_{obs}, kJ/mol[1]) against IP800 concentration (mM). All experiments were repeated twice to achieve reproducibility within ±2%.

2.2.6. Nuclear Magnetic Resonance, ^{1}H NMR. The NMR experiments were conducted on a Bruker Avance 600 spectrometer with a ^{1}H frequency of 600.13 MHz. Temperature was kept constant within ±0.1 °C by using a Bruker BCU-05 temperature control unit. The samples were allowed to equilibrate at the desired temperature for at least 10 min before measurement. A total of 32 times of accumulation were acquired generally. DSS was used to eliminate the temperature-induced shifts. A stock solution of 0.025 M DSS in water was prepared, and 14 μL of stock solution of DSS was injected into 0.7 mL of IP800/PEG aqueous solutions with a syringe, so that the final solutions contained 0.5×10^{-3} M DSS. D_2O (>99.5%) was used as solvent.

3. Results

3.1. IP800/Water System. The surface tension γ is plotted as a function of IP800 concentration in the presence and absence of 5.00 wt % PEG400 and PEG20000 (Figure 1). The surface tension decreases sharply in the beginning and then levels off beyond an IP800 concentration of 0.45 mM (critical micelle concentration, cmc), indicating full absorption of IP800 molecules on the surface and formation of micelles in the solution. The presence of PEG reduces slightly the surface tension of IP800 at low IP800 concentrations, but the critical concentration

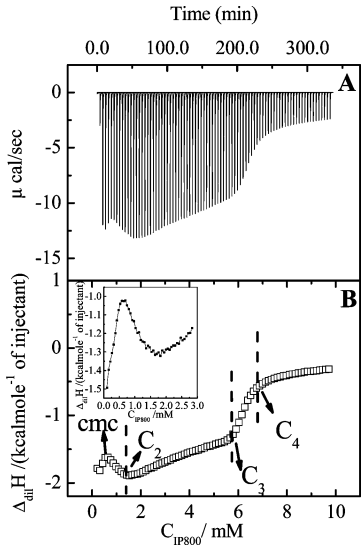

Figure 2. Calorimetric titration curves of IP800 solution in water, C_{IP800} = 51.73 mM. Inset: curve of different IP800 concentrations in water, C_{IP800} = 14.85 mM.

(cmc) and the value of the equilibrium surface tension are nearly identical to those of the pure IP800 solution.[18]

Isothermal titration calorimetry (ITC) is one of the most sensitive techniques that permits direct measurement of thermodynamic changes in the course of binding and micellization. Figure 2 shows experimental data obtained by ITC measurements as a function of time and of IP800 concentration. From Figure 2A, it can be noted that the dilution of IP800 micellar solution is exothermic in the concentration range investigated. At low IP800 concentrations (Figure 2B, inset), the enthalpy curve corresponding to the titration of micellar IP800 shows an exothermic decrease leading to a first exothermic minimum (−1.622 kJ/mol) at about 0.43 mM (cmc); a subsequent smooth exothermic maximum (−1.885 kJ/mol) at 1.65 mM (defined as C_2, represents the IP800 concentration at the beginning of the interaction of inter-IP800 aggregates) follows; with further addition of IP800, a huge endothermic progress reflected in enthalpy occurs at 5.78 mM (defined as C_3, represents the IP800 concentration at the formation of the relatively small IP800 micelles), until the IP800 concentration further increases to 6.88 mM (defined as C_4, represents the IP800 concentration at IP800 aggregates with fixed microstructure), from which the enthalpy curve reaches a plateau (−0.322 kJ/mol).

Figure 3A shows the clouding temperature (T_c) as a function of IP800 concentration. The T_c values cannot be detected in the temperature range above 90 °C at relatively low IP800 concentrations (<cmc), and the results are not shown. From Figure 3A, we can find that the clouding temperature decreases with IP800 concentration at first and reaches a minimum at 1.01 mM (∼C_2), and then increases rapidly, until the concentration reaches 4.93 mM (∼C_3); from there on, the increase of the clouding temperature becomes smooth and, finally, tends to constant beyond 10.50 mM (∼C_4). The value of C obtained by the ITC method is much more accurate than the clouding temperature observed visually. So the discussions at different C values are based on the results obtained by the ITC method and are supported by the results of the clouding temperature. Using pyrene as a probe,[26–28] the intensity ratio of the first peak to the third (I_1/I_3) of pyrene emission spectra shows the polarity and hence the location of pyrene probe molecules in the micelles.[26] As can be seen in Figure 3B, the intensity ratio exhibits a sharp decrease with increasing IP800 concentration at first. However, unexpectedly, beyond the cmc, the value of the ratio exhibits a maximum peak around C_2 and then finally reaches an approximate constant.

Förster theory[23,29] proposes that resonance energy transfer occurs by a dipole−dipole long-range coupling interaction which depends on certain spectroscopic and geometric properties of the donor−acceptor pair. In the present experiment, ANS is selected as energy acceptor and IP800 itself as energy donor. The extent of spectral overlap between the donor emission and acceptor absorption is shown in the Supporting Information (Figure S2). The fluorescence resonance energy transfer investigation can provide the information about the distance between IP800 and ANS, which indicates the microstructure of IP800 aggregates and the effect by the addition of PEG. The relative fluorescence intensity in the absence (a) and presence (b) of ANS[23,29] is presented in Figure 4A. The intensity shows a maximum; comparing line (a) and line (b), it can be seen that the addition of ANS causes the intensity value to decrease, revealing that the energy transfer occurs between IP800 and ANS.[23] The energy transfer efficiency (E_T) can be calculated via the equation $E_T = 1 - F/F_0$, where F_0 and F represent the florescence intensity in the absence and presence of probe ANS, respectively, and the results are shown in Figure 4B. The change of the E_T value with IP800 concentration exhibits the shape of "M", and the concentrations of transfer points correspond to the cmc, C_2, and C_3.

Dynamic light scattering (DLS) provides a noninvasive means of probing conformational changes. Hence, the relaxation time distributions of IP800 in aqueous solution at different concentrations obtained by DLS measurements are shown in Figure 5A, and the hydrodynamic radii are shown in Figure 5B. The shed light is too weak to measure at low IP800 concentrations (≤0.3 mM, results not shown), revealing that no aggregates formed. Only one peak corresponding to the translational diffusion of IP800 micelles is evident until the IP800 concentration reaches 0.78 mM, where the relaxation time distribution exhibits two distinct peaks, indicating a more polydisperse size distribution. The average hydrodynamic radii of IP800 aggregates increase with IP800 concentration at lower IP800 concentration range (<C_2). The hydrophilic segment of IP800 has about 16−18 CH_2-CH_2-O monomers, and the chain contour length is about 3.24 nm (monomer length about 0.18 nm);[22] it should be safe to assume that the radius of IP800 micelles is approximately 3.24 nm, which is much smaller than the experimental value (>30 nm). To verify the morphology of the clusters, the FF-TEM result (Figure S3 in the Supporting Information) reveals that the clusters are mainly spherical, coupling with some irregular morphologies. When the IP800 concentration enters into the range between C_2 and C_3, the clouding temperature is lower than room temperature (25 °C) (Figure 3A), and the size of the IP800 aggregates represents as a radical change (about 200 nm). For IP800 concentrations beyond 15 mM, the relaxation time distributions exhibit only one peak corresponding to the hydrodynamic radii of 5.0 nm, well consistent with the calculated value, and it is not dependent on IP800 concentration anymore (Figure 5B).

3.2. IP800/ PEG/water system. ***3.2.1. Constant IP800 Concentration and Varying PEG Molecular Weight.*** For the ternary system of IP800/PEG/water, the binding interaction between PEG and IP800 is investigated by isothermal titration calorimetry (ITC). Figure 6 shows the titration curve of an IP800 micellar solution in 5.0 wt % PEG aqueous solutions with different molecular weights (MWs). Deviations from IP800 micellar solution titrated into water indicate that the interaction

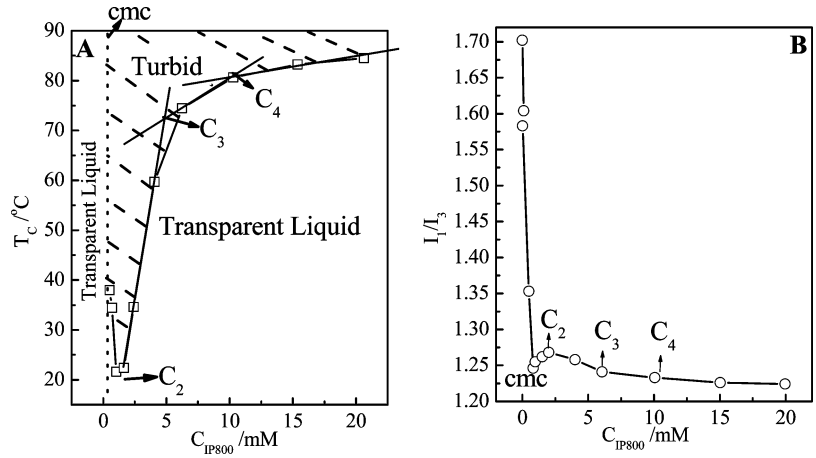

Figure 3. Clouding temperature (A) and pyrene I_1/I_3 ratios (B) as a function of IP800 concentration.

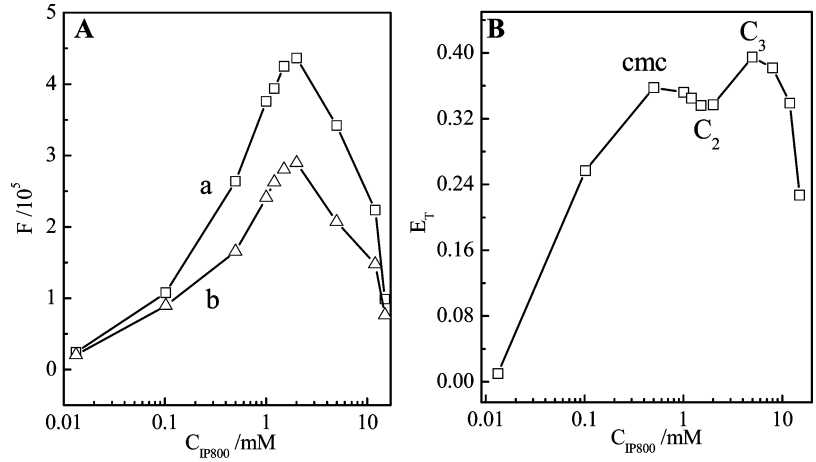

Figure 4. (A) Fluorescence intensity of IP800 in the absence (a) and presence (b) of ANS; (B) energy transfer efficiency (E_T) between IP800 and ANS.

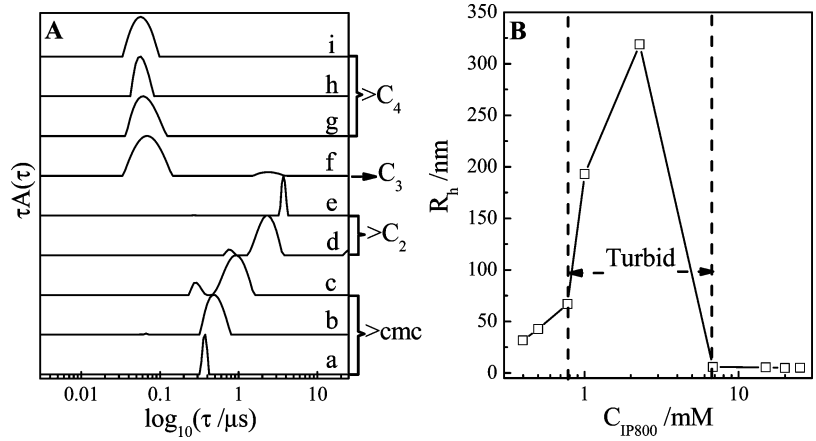

Figure 5. (A) DLS measurements of the size distributions of IP800 in water at concentrations of (a) 0.40, (b) 0.50, (c) 0.78, (d) 1.002, (e) 2.283, (f) 6.783, (g) 15.03, (h) 20.01, and (i) 25.05 mM. (B) Hydrodynamic radius, R_h with IP800 concentration.

between PEG and IP800 occurs even at the lowest IP800 concentrations measured, and there is no significant difference among PEGs with different MWs. When the IP800 concentration reaches C_4, the enthalpy curves of PEG/IP800/water merge with each other (−0.322 kJ/mol) but appear a little smaller than that of IP800/water (−0.409 kJ/mol). Besides, the addition of PEG has no effect on the cmc of IP800, which agrees with the results of surface tension investigations; however, C_2 and C_3 shift to higher IP800 concentrations with increasing MW_{PEG}.

To investigate the effect of MW_{PEG} on the morphology of relatively larger micelles of IP800, the concentration of IP800 is fixed at 0.5 mM and the concentration of PEG is fixed at 5.0 wt %. Figure 7A shows the changes in the relaxation time distributions for the PEG/IP800/water system with varying MW_{PEG}. As shown in section 3.1, the distribution is unimodal in pure IP800 solution at 0.5 mM; the addition of PEG drives the distribution to split into two well-separated and well-defined components. The corresponding hydrodynamic radii are listed in Table 1. From Figure 7A and Table 1, it can be noted that the relaxation time distributions and the size of the fast peak increase with MW_{PEG}. Compared with the pure PEG/water system,[23,30] the fast mode is identical to PEG random coil, so

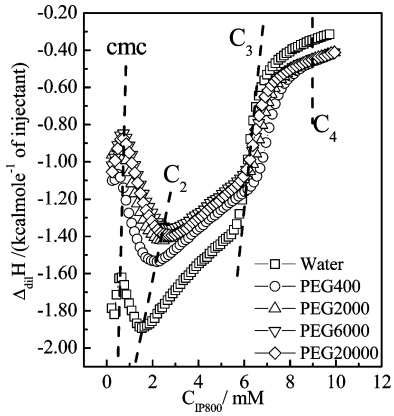

Figure 6. Enthalpy change as a function of surfactant concentration due to the titration of micellar IP800 into 5.00 wt % PEG solutions with different molecular weights. $C_{IP800} = 58.00$ mM.

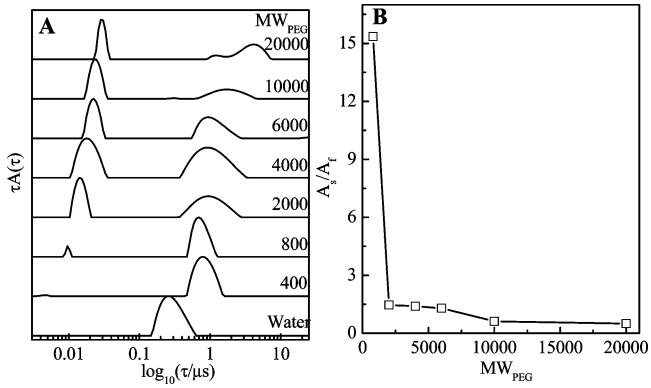

Figure 7. Relaxation time distributions for the ternary IP800/PEG/water system at different MW_{PEG} values, $C_{IP800} = 0.5$ mM, $w_{PEG} = 5.0$ wt % (A); dependence of the slow to the fast mode relation amplitude, A_s/A_f as a function of MW_{PEG} (B).

TABLE 1: Hydrodynamic Radius, R_h, of PEG/Water System and IP800/PEG/Water System with Different Molecular Weights of PEG (MW_{PEG})[a]

	PEG/water	IBF-PEG800/PEG/water[a]	
MW_{PEG}	R_h (nm)[b]	R_h (fast) (nm)	R_h (slow) (nm)
0			21.47
400	0.42	0.51	63.96
800	0.65	0.82	58.02
2000	0.91	1.21	80.56
4000	1.29	1.52	80.56
6000	1.58	1.93	118.86
10000	2.00	2.08	138.87
20000	2.90	2.63	162.22

[a] $C_{IP800} = 0.5$ mM; $w_{PEG} = 5$ wt %. [b] The values were calculated by using the equation in ref 40.

the fast mode represents the single PEG random coil. And the relaxation time distributions and the size of the slow mode are much higher than those of IP800 micelles, which correspond to IP800/PEG complexes. The dependence on PEG concentration of the ratio of the slow to fast mode relative amplitudes, A_s/A_f, for the ternary system is presented in Figure 7B. Combining Figure 7B and Table 1, we can find that, at the fixed concentration of IP800 and PEG, the A_s/A_f ratio decreases sharply with PEG molecular weight at first until the MW_{PEG} is up to 2000, and the hydrodynamic radii of the complexes are also enlarged. The value of A_s/A_f becomes independent of MW_{PEG} in the range of 2000−6000, as the size of the complexes does; and the A_s/A_f value shows a slightly further decrease when

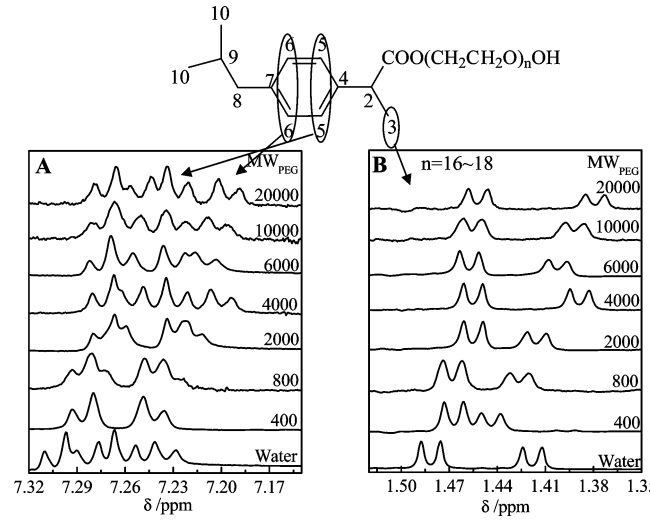

Figure 8. ^{1}H NMR signals of phenyl protons H5 and H6 (A) and proton H3 (B) of IP800 in the presence of 5 wt % PEG with different molecular weights, $C_{IP800} = 0.50$ mM.

MW_{PEG} is raised to 10 000, revealing that the IP800/PEG800 complex contribution to the total scattered intensity is less with respect to the PEG coil.

^{1}H NMR can provide the intrinsic quality of self-assembly, which is used to determine the interaction mechanism of PEG and IP800 forming IP800/PEG complexes. Figure 8 shows the ^{1}H NMR signals of phenyl protons H5 and H6 (Figure 8A) and proton H3 (Figure 8B) of IP800 in the presence and absence of PEG with different MWs, respectively. From Figure 8A, the addition of PEG with MW from 400 to 2000 induces a dramatic change in the hyperfine structure of the H5 and H6 protons, and this effect increases with decreasing MW_{PEG}; however, the hyperfine structure is not affected by PEG with MW beyond 2000. As shown in Figure S1 in the Supporting Information, the chemical shift of proton H3 is about 1.45 ppm in $CDCl_3$, but two signals appear in this range in the aqueous solution investigated. The signals at the lower field are attributed to proton H3 of IP800 micelles, and those at the higher field correspond to those of IP800 monomers (Figure 8B). The signals of proton H3 of IP800 micelles and monomers both exhibit significant chemical shifts upon addition of PEG with MWs ranging from 400 to 2000 (Figure 8B). As shown in Figure S4 in the Supporting Information, the chemical shift of IP800 monomers exhibits an upfield shift with the addition of PEG in this region and becomes prominent with the increase of MW_{PEG}; the effect of PEG addition becomes stable as MW_{PEG} further increases (>2000). For proton H3 of IP800 micelles, the chemical shift exhibits a downfield shift, but the effect of that decreases with MW_{PEG} from 400 to 2000; for MW_{PEG} ranging from 2000 to 6000, the chemical shift exhibits an upfield shift with increasing MW_{PEG}, and the effect of the addition of PEG exhibits a slight increase with MW_{PEG} from 6000 to 20 000.

3.2.2. Constant IP800 Concentration and Varying PEG Concentration. According to the effect of different MW_{PEG} values on the microstructure of the complexes, we chose PEG400 and PEG20000 which interact with IP800 micelles by totally different models to investigate the effect of PEG concentration on the microstructure of the complexes. The effect of PEG concentration on the heat exchange upon interaction with titrated micellar IP800 was also evaluated. Figure 9 shows enthalpy change as a function of IP800 concentration due to the titration of IP800 micellar solutions into PEG400 (A) and PEG20000 (B) aqueous solutions at different concentrations. It

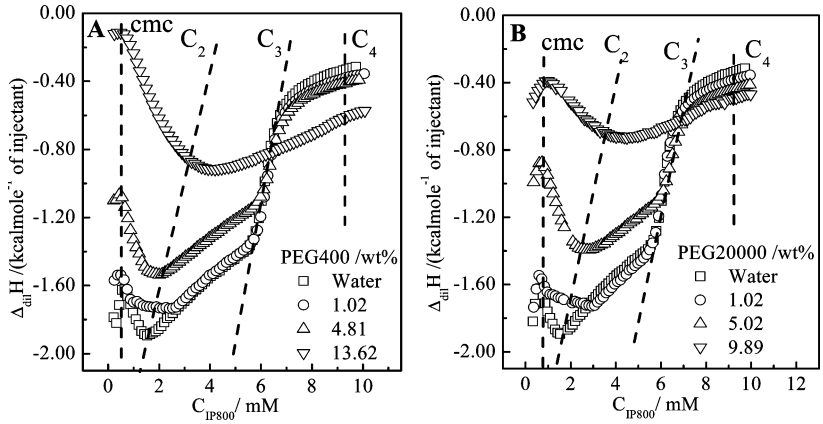

Figure 9. Enthalpy change as a function of surfactant concentration due to the titration of IP800 micellar solutions in 5.00 wt % PEG with MW_{PEG} = 400 (A) and 20 000 (B); C_{IP800} = 58.00 mM.

TABLE 2: Critical Concentration of IP800, C_2 and C_3, in IP800/PEG/Water System with Different Concentrations of PEG400 and PEG20000

	IP800/PEG400/water		IP800/PEG20000/water	
w_{PEG} (wt %)	C_2	C_3	C_2	C_3
0	1.532	5.435	1.532	5.435
1	1.71	5.722	1.95	5.504
5	1.889	5.984	2.601	5.976
10	3.931		4.135	

is evident that an increase in polymer concentration does not affect the value of the cmc but causes an increase of the positions of C_2 and C_3 (Table 2). Moreover, an increase of the maximum (from −1.621 to −0.113 kJ/mol) and a broadening of the endothermic peak are obviously observed. As IP800 concentration further increases upon C_4, the enthalpy plateau exhibits a gradual decrease with PEG400 concentration. For the PEG20000/IP800/water system, the effect of the addition of PEG is similar to that of PEG400 (Figure 9B).

Figure 10A and B shows the effect of PEG400 and PEG20000 concentration on the relaxation time distributions in the ternary IP800/PEG/water system. In the IP800/PEG400/water system, at a given IP800 concentration (0.5 mM) (Figure 10A), the fast mode is similar to that of pure IP800 solution and the relative amplitude of the slow mode associated with IP800/PEG complexes increases significantly as PEG concentration is increased at first, indicating a rising amount of the complexes. When PEG concentration is up to 1.0 wt %, the distribution peak appears as broad and unimodal. The distribution peak becomes narrow when PEG concentration is over 1.5 wt %, and then the shape of peak is essentially independent of PEG concentration, suggesting that the interaction between IP800 and PEG reaches saturation. In IP800/PEG20000/water system, the addition of PEG20000 drives the distribution to split into two well-defined components, fast and slow mode. However, different from the case of PEG400, the fast mode is much smaller than that in the IP800/water system. And it decreases with PEG20000 concentration, which is identical to pure PEG20000, so it is attributed to PEG20000 random coil.[31] Besides, the slow mode associated with IP800/PEG20000 complexes increases with PEG20000 concentration, but the intensity decreases. Figure 10C illustrates the change of the ratio of the slow to fast mode relaxation amplitudes (A_s/A_f) with changing PEG20000 concentration at constant IP800 concentration. The ratio value decreases strongly with PEG20000 concentration first, but then the variation of the ratio becomes negligible as the concentration

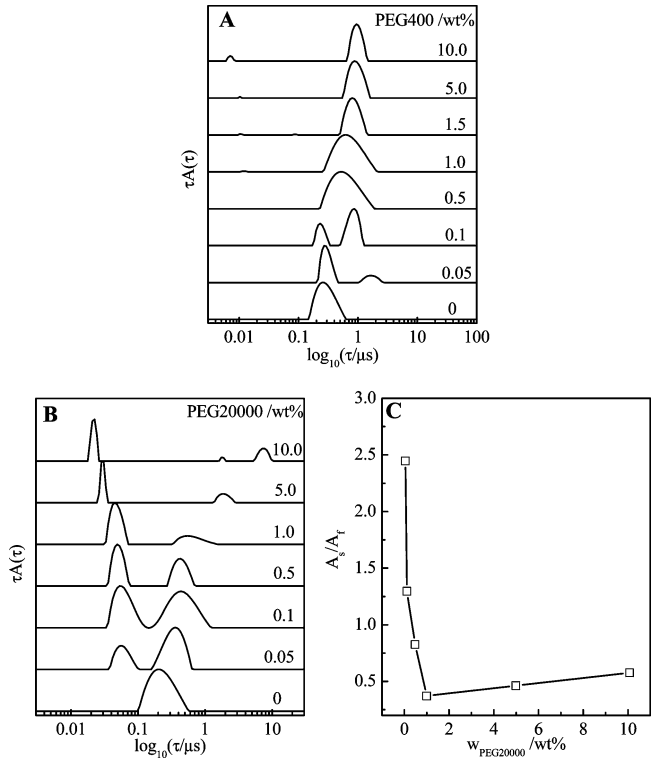

Figure 10. Relaxation time distributions for the ternary IP800/PEG/water system with concentration of increasing PEG400 (A) and PEG20000 (B); dependence of the slow to the fast mode relation amplitude, A_s/A_f (C) for the system with PEG concentration, C_{IP800} = 0.50 mM.

of PEG20000 is up to 0.8 wt %, indicating that PEG random coil contributes the main part to the total scattered intensity.

According to our ^{1}H NMR investigation on the effect of PEG molecular weight (MW_{PEG}) on the microstructure of the complexes, the addition of relatively short PEG chains can affect the microenvironment of hydrophobic segment protons of IP800, especially proton H3 which is located at the interface between the hydrophilic corona and hydrophobic core (corona−core interface). Figure 11 shows the ^{1}H NMR signal change of phenyl protons H5, H6 and H3 of IP800 with PEG400 and PEG20000 concentrations. The addition of a small amount of PEG400 strongly changes the hyperfine structure of H5 and H6 (Figure 11A), but the hyperfine structure of them does not change anymore with PEG400 concentration beyond 5 wt %. In addition, Figure 11B shows that the chemical shift of H3 in IP800 micelles exhibits a significant downfield shift, and for

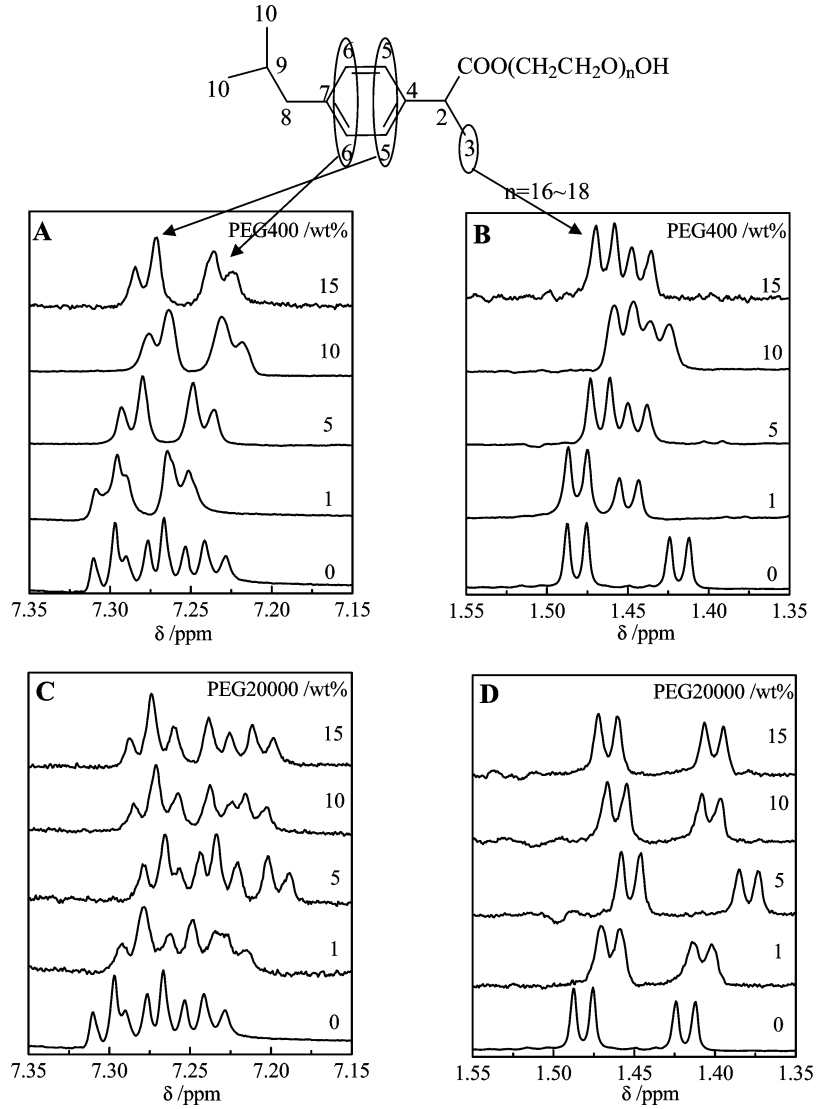

Figure 11. ^{1}H NMR signals of phenyl protons H5 and H6 (A, C) and proton H3 (B, D) of IP800 in the presence of PEG with different concentrations/(wt %), $C_{IP800} = 0.50$ mM.

the chemical shift of H3 of IP800 monomers an upfield shift is observed (Figure S5A in the Supporting Information). In the system of IP800/PEG20000/water, the proton H3 of IP800 as monomers or in micelles exhibits a slight upfield shift (Figure 11C, D and Figure S5B in the Supporting Information).

Figure 12 shows the energy transfer efficiency in IP800/PEG/water systems as a function of PEG concentration. In IP800/PEG400/water system, the value of E_T declines with PEG concentrations at first until up to 1.0 wt %, and then the value becomes constant. In the IP800/PEG20000/water system, a similar initial decrease is observed, but the value of E_T rises slightly after PEG20000 concentration is raised above 0.8 wt %.

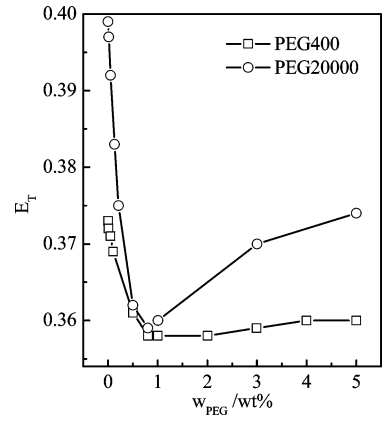

Figure 12. Energy transfer efficiency in IP800/PEG/water system as a function of PEG concentration, $C_{IP800} = 0.50$ mM.

4. Discussion

4.1. The Aggregation and Morphology of IP800 in an Aqueous System. For the binary system of IP800/water in the present paper, the heat of dilution plays a very important role, showing that the system investigated is exothermic (Figure 2A). In the beginning, as the micellar solutions of IP800 titrate into water, two processes, dimicellization as an endothermic process and hydration as an exothermic process, are involved. Beyond the cmc of 0.48 mM, the hydrophobic interaction drives IP800 monomers to aggregate, followed by dehydration of IP800. This progress displays a clear exothermic minimum (Figure 2B). As soon as IP800 micelles form, the probe ANS can penetrate into IP800 micelles, and then the acceptor ANS and the donor IP800 molecules become much closer to each other, which results in the initial distinct increase of energy transfer efficiency (Figure 4A). In addition, pyrene is dissolved into the hydrophobic core

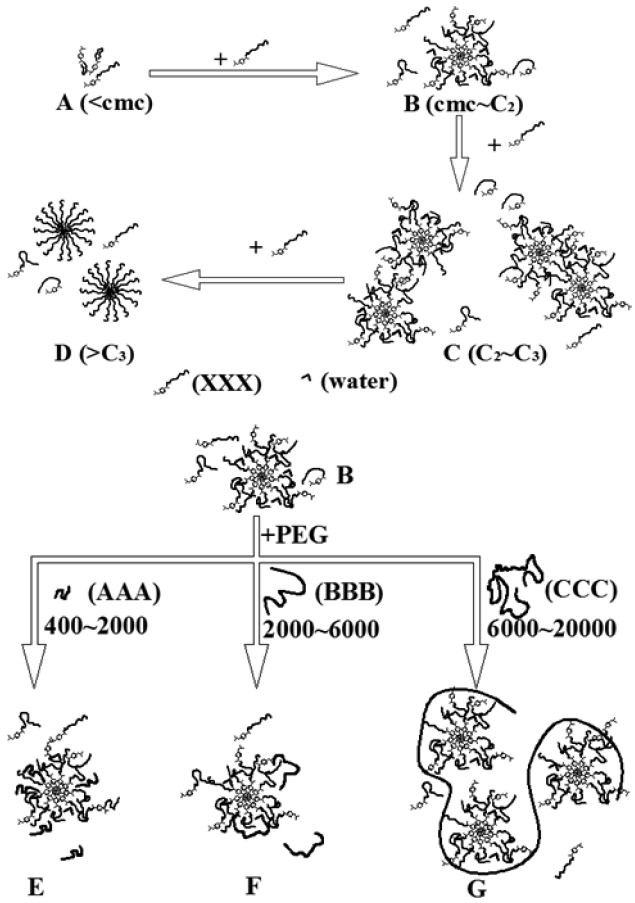

Figure 13. Illustration of the structure transition of IP800 micelles with IP800 concentration and IP800/PEG complexes with different MW_{PEG} values. **XXX** is presented as IP800 molecule; **AAA**, **BBB**, and **CCC** are presented as PEG chains with different MWs.

of IP800 micelles where the polarity of the microenvironment is relatively lower than that of the water phase,[26,27] so the value of I_1/I_3 declines sharply with the formation of IP800 micelles (Figure 4B).

The hydrophilic segments of IP800 appear neutral, flexible, and of low polydispersity. They can fold and form corona shells of IP800 micelles with many water molecules penetrating. The looser corona layer of the micelles facilitates IP800 monomers in the bulk to bind on the surface of the micelles[24] (Figure 13B), with the result that the value of the hydrodynamic radii of IP800 micelles is relatively big (about 30 nm) (Figure 5A, a−c and Figure S3 in the Supporting Information) in this concentration region. The hydrophobic segment of IP800 binding on the surface makes the surface free energy rather high, which induces the clouding temperature of the system to decline (Figure 3A). Moreover, the absorption of IP800 brings about the variation of the microenvironment of the probe pyrene and drives the solubilized pyrene to move to the outer side of the IP800 micelles, showing an interesting increase of the I_1/I_3 value around cmc-C_2 (Figure 3B). And the distance between ANS and IP800 becomes larger, resulting in the decline of the E_T value (Figure 4B).

Borisov and Halperin[32] propose that the polysoaps can form intrachain micelles resulting from the exchange of amphiphiles between them. In the present experiment, the unfolded EO chain of IP800 micelles can penetrate into another IP800 micelle with IP800 concentration from C_2 to C_3. Meanwhile, the hydrophobic segments of IP800 binding on the surface of IP800 micelles can interact with each other and then form bigger aggregates (Figure 13C) to reduce the relatively high interfacial energy of the water-hydrophobic interface.[33] The onset of bridging interaction will drive the hydrophilic segment of IP800 monomers binding on the micelle surfaces outside and then each aggregate becomes a little tighter; thus, the inner polarity decreases again inflected by the location of probe pyrene, and the energy transfer efficiency (E_T) increases.

In the region of C_3 to C_4, the hydrophobic force drives IP800 micelles to be much tighter, followed by further dehydration of the hydrophilic segment of IP800 micelles, which exhibits a big endothermic progress (Figure 2B). The number of binding positions for IP800 monomers gets smaller with the shrinkage of IP800 micelles, which leads IP800 monomers to release and the multiaggregates to disassociate. So the size of the aggregates becomes smaller (Figure 5A, d−f), and the interfacial energy of IP800 micelles declines efficiently, which is affirmed by a sudden increase of clouding temperature. In addition, IP800 and ANS get closer to each other by IP800 micelle shrinkage, which causes the value of E_T to increase; on the other hand, the pyrene molecules are solubilized into the core again showing that the value of I_1/I_3 tends to stability (Figure 3).

Eventually, with IP800 concentration beyond C_4, IP800 molecules form relatively small and tight micelles for the shrinkage of IP800 micelles (Figure 5A, d−f and Figure 13D). In this region, the progress involving the titration of IP800 micellar solution into water is simply dilution of micelles displaying a plateau exothermic thermogram. This means that the microstructure of IP800 micelles does not change any more with IP800 concentration and only dilution of IP800 micelles is involved. The radius of IP800 micelles measured by light scattering (5 nm) (Figure 5.\) agrees well with the calculated value corresponding to the chain length of IP800, so it is safe to conclude that well-defined spherical micelles are formed. The polarity of the microenvironment (Figure 3B) becomes constant, which also confirms the explanation above. However, the inner filter effect of IP800 micelles may be the dominant progress at higher concentrations,[30] which makes the value of E_T decrease significantly (Figure 4A).

4.2. The Effect of the Molecular Weight of PEG on the Configuration of the IP800/PEG Complex. The interaction of EO chains, hydrogen bonding of $-CH_2-O-$ and hydrophobic force of $-CH_2-$, between IP800 molecules and PEGs drives them to interact with each other,[24,34] even though IP800 molecules exist as monomer. The results of ITC experiments verify this explanation. The attachment of the segments of the PEG coil to IP800 micelles interferes with hydrogen bonding, resulting in partial dehydration of those segments,[19] which displays an endothermic progress in the thermogram of the IP800/PEG/water system. And the amount of the reduced heat is not regularly sensitive to MW_{PEG} (Figure 5). Since IP800 monomers aggregate as relatively looser micelles, the PEG coil as an amphiphilic character[14] can penetrate into or drape around the micelles. This kind of binding changes the microstructure of IP800 micelles and enlarges the distance between IP800 molecules and ANS penetrated, resulting in a decrease of E_T (Figure 12). If hydrophilic PEG penetrates into the core of IP800 micelles, the micelle core would experience a different environment. Consequently, the chemical shift of the proton in the core should be rather different in the corresponding solution with and without PEG.[35,36] In the present paper, the protons of the hydrocarbon of IP800 in the micelles tend to move downfield, especially proton H3 which stays at the corona−core interface (Figure 8, Figure S4 in the Supporting Information). In addition, the downfield chemical shift of C−H protons of the PEG

segment should have been observed, which is related to the formation of hydrogen bonds of PEG with hydrophilic segments of IP800. However, in the IP800/PEG/water system, the results are not shown because of the overlap signals from EO chains of PEG molecules with the hydrophilic segment of IP800 molecules.[23] Besides, the protons of IP800 hydrocarbon display a significantly upfield shift with increasing MW_{PEG}, since the hydrophilicity of PEG decreases with increasing PEG chain length, which induces the solvent quality to decline.

At a fixed weight fraction of PEG, the amount of PEG chains decreases with MW, which brings fewer terminal hydroxyls by which hydrogen bonds can form much more easily. Moreover, the PEG chain penetrates into IP800 micelles more easily with a decrease of MW_{PEG} because of the relatively low space hindrance effect. For these reasons, the amount of PEG chains interacting with IP800 micelles increases with the decrease of MW_{PEG} at a fixed weight fraction, showing that the isolated PEG coil contributing to total intensity increases with MW_{PEG} (Figure 7). Furthermore, these explanations also are verified by the results of the cloud point investigation that the cloud point decreases with an increase of the amount of PEG chains interacting with IP800 micelles.[33]

For PEG with MW less than 2000, PEG chains can penetrate deep into relatively looser IP800 micelles and even to the corona−core interface of IP800 micelles (Figure 13E), resulting in a change of microenvironment of the complex core. The explanation is consistent with the results of ^{1}H NMR (Figure 8): the chemical shift of proton H3 which stays at the corona−core interface exhibits a more significant downfield shift than other hydrocarbon protons of IP800 molecules. And this effect decreases with MW_{PEG} due to the space hindrance effect. Moreover, the amount of PEG which interacts with IP800 micelles decreases with MW_{PEG} as mentioned before, which coincides with the increase of the size of IP800/PEG complexes (Table 1 and Figure 7). For PEG with MW higher than 2000, PEG chains cannot penetrate deep into the micelles because of the space hindrance effect and few terminal hydroxyls, but bind at the surface of micelles or drape around the micelles. Thus, a lesser effect on the microenvironment of the IP800 micelle core is observed (Figure 8). Within the MW_{PEG} range from 2000 to 6000 (Figure 13F), the essential feature of this model is opposed by the high excluded volume energies resulting from localization of the absorbed chain to a finite volume of space.[33] Thus, the size of the complexes in this region slightly increases with MW_{PEG} (Figure 7), and the slow mode contributing to the total intensity tends to be constant. For MW_{PEG} beyond 6000 (Figure 13G), the PEG chain is long enough to wrap around several micelles,[23] so a sudden rise can be observed in the size of the complexes (Table 1), and a sudden decline of the slow mode contributing to the total intensity is induced (Figure 7B).

In addition, since the free and relatively small IP800 micelles form at IP800 concentrations higher than C_3, the relatively looser complexes which are formed as PEG penetrates into looser IP800 micelles are broken down and the rehydration of PEG is expelled from the micelle to water.[14] Thus, these rehydrated PEG segments wrap around IP800 micelles independent of MW_{PEG}, causing part of PEG to dehydrate again, showing a slight decline of the heat in the thermogram of the IP800/PEG/water system compared with the IP800/water system.

4.3. The Effect of PEG Concentration on the Binding Characteristics between PEG and IP800. To explore the effect of PEG concentration on the binding characteristics between IP800 and PEG, two different binding models were chosen. With increasing PEG concentration, the binding reactions increase proportionately. This leads to an increase in the binding enthalpy changes as indicated by the increase in the area of the endothermic curve (Figure 9). The same was already noticed in previous investigations;[22] an increase in polymer concentration does not affect the value of the cmc, suggesting that the aggregates rather than monomers induce the interaction between IP800 and PEG and the excluded volume is the driving force for complexation. And in this experiment it causes an increase of C_2 and C_3 (Table 2), which gradually shift to larger values, indicating a proportionally large concentration of surfactant binding to the polymer.

Furthermore, when the concentration of PEG is relatively low (1.0 wt %) (Figure 9), a relatively small amount of IP800 is needed to saturate. As IP800 concentration further increases, the heat curve merges with that of the pure IP800 solution.

According to the investigation above, PEG400 penetrates deep into IP800 looser micelles (Figure 13G) at a fixed IP800 concentration. Hence, the polarity of the microenvironment of IP800 micelle cores rises with the addition of PEG. When PEG400 chains have not saturated IP800 micelles, isolated IP800 micelles still exist in the system, showing an isolated and well-defined distribution peak observed in Figure 10A. And in this region the effect on micropolarity of IP800 micelles increases with PEG concentration. Since PEG saturates IP800 micelles, the microstructure of IP800/PEG400 complexes does not change anymore (Figure 11 and Figure S5A in the Supporting Information). From the result of energy transfer efficiency, the saturation concentration of PEG400 binding to IP800 micelles is 1.0 wt %. The results can be confirmed by DLS measurement, which displays a narrow peak, and the value of the size does not change with PEG400 concentration anymore at PEG concentrations higher than 1.5 wt %. From the steady fluorescence experiment,[37−39] the aggregation number of IP800 micelles at this concentration is about 90. According to ^{1}H NMR spectra, the number of IP800 micelles in the system can be determined. Assuming that PEG400 chains completely bind with IP800 micelles at saturation and that the aggregation number of IP800 does not change in the presence of PEG400, the ratio of PEG400 to IP800 micelles is about 15:1.

When MW_{PEG} changes from 400 to 20 000, PEG chains mainly wrap around the IP800 micelles (Figure 13H). Dramatically different from the case of PEG400, PEG20000 chains just wrap around IP800 micelles because of a huge space hindrance effect. Therefore, the microenvironment of IP800 micelles does not exhibit obvious difference with pure IP800 micelles (Figure 11C, D and Figure S5B in the Supporting Information). However, the addition of PEG still enlarges the distance between IP800 and penetrating ANS because of the terminal hydroxyls of PEG20000, showing the declining value of E_T (Figure 12). Moreover, the size of the complexes is about 3−4 times that of IP800 micelles, since PEG20000 chains can wrap several IP800 micelles (Figure 10B and Table 1), causing the inner filter effect to decline (Figure 12). PEG20000 wrapping around IP800 micelles is in equilibrium with PEG20000 in the bulk. Thus, the isolated PEG coil exists below the saturation PEG20000 concentration (Figure 10B). When the PEG chain saturates an IP800 micelle, a more isolated PEG20000 coil forms with a further increase of PEG20000 concentration, and the slow mode intensity attributing to IP800/PEG complexes becomes much smaller (Figure 10C). And the saturation concentration of PEG20000 interacting with IP800 is about 0.8 wt %, obtained by the energy transfer efficiency investigation.

5. Conclusion

Hydrophilic modification of ibuprofen with 16−18 monomers of EO is obtained as a functional surfactant. The aggregation of IP800 strongly depends on its concentration: within the concentration range cmc to C_2, it can form looser micelles and IP800 monomers in the bulk can bind on the micelles surface; the micelles interact with each other by intrachain interaction at C_2 to C_3; when IP800 concentration is beyond C_3, IP800 monomers start to form relatively smaller micelles; and the structure of IP800 micelles become stable and well-defined at IP800 concentrations higher than C_4.

The binding models of looser IP800 micelles and PEG strongly depend on the molecular weight of PEG (MW_{PEG}): for MW_{PEG} less than 2000, PEG chain can penetrate into the corona−core interface of IP800 micelles; the PEG chain binds onto the surface of IP800 micelles with a MW_{PEG} range from 2000 to 6000; and as the MW of PEG is greater than 6000, one chain can wrap around several IP800 micelles. The saturation ratio of PEG400 to IP800 micelle at a fixed IP800 concentration is 15:1, and one PEG20000 chain can interact with three to four IP800 micelles. A relatively higher molecular weight of PEGs will improve the stability of the IP800 aqueous solution.

Acknowledgment. This work was financially supported by the National Nature Science Foundation of China (Nos. 20633010 and 20773106).

Supporting Information Available: ^{1}H NMR and ^{13}C NMR spectra of IP800 in $CDCl_3$ (Figure S1). Absorption spectrum of ANS in IP800 solution and emission spectrum of IP800 in aqueous solution (Figure S2). FF-TEM of the system of IP800/water with C_{IP800} = 0.5 mM (Figure S3). Chemical shift variations ($\Delta\delta$H) (B) of proton H3 of IP800 monomers and micelles in the system of IP800/PEG/water with different molecular weights of PEG (Figure S4). IP800/PEG400 and PEG20000/water at different concentrations, C_{IP800} = 0.5 mM (Figure S5). This material is available free of charge via the Internet at http://pubs.acs.org.

References and Notes

(1) Schuller, H. M.; Zhang, L.; Weddle, D. L.; Castonguay, A.; Walker, K.; Miller, M. S. *J. Cancer Res. Clin. Oncol.* **2002**, *128*, 525.
(2) Buser, H. R.; Poiger, T.; Müller, M. D. *Environ. Sci. Technol.* **1999**, *33*, 2529.
(3) Henry, D.; Lim, L. L.; Garcia, R. L. A.; Gutthann, P. S.; Carson, J. L.; Griffin, M.; Savage, R.; Logan, R.; Moride, Y.; Hawkey, C.; Hill, S.; Fries, J. T. *BMJ* **1996**, *312*, 1563.
(4) Stephenson, B. C.; Rangel-Yagui, C. O.; Junior, A. P.; Tavares, L. C.; Beers, K.; Blankschtein, D. *Langmuir* **2006**, *22*, 1514.
(5) Hussein, K.; Türk, M.; Wahl, M. A. *Pharm. Res.* **2007**, *24*, 585.
(6) Desjardins, P.; Black, P.; Papageorge, M.; Norwood, T.; Shen, D. D.; Norris, L.; Ardia, A. *Eur J. Clin. Pharmacol.* **2002**, *58*, 387.
(7) Pawar, A. P.; Paradkar, A. R.; Kadam, S. S.; Mahadik, K. R. *AAPS Pharm. Sci. Tech.* **2004**, *5*, 44.
(8) Gavrilin, M. V.; Ushakova, L. S.; Karpenya, L. I. *Pharm. Chem. J.* **2003**, *37*, 31.
(9) Bhat, P. A.; Dar, A. A.; Rather, G. M. *J. Chem. Eng. Data* **2008**, *53*, 1271.
(10) Lee, C. W. *Macromol. Res.* **2004**, *12*, 63–70.
(11) Anikina, L. V.; Levit, G. L.; Demin, A. M. V.; Vikharev, Yu. B.; Safin, V. A.; Matveeva, T. V.; Krasnov, V. P. *Pharm. Chem. J.* **2002**, *36*, 237.
(12) Mehlisch, D. R.; Ardia, A.; Pallotta, T. *Curr. Ther. Res.* **2003**, *64*, 327.
(13) Yan, H.; Kawamitsu, H.; Kushi, Y.; Kuwajima, T.; Ishii, K.; Toshima, N. *J. Colloid Interface Sci.* **2007**, *315*, 94.
(14) Dai, S.; Tam, K. C. *J. Phys. Chem. B* **2001**, *105*, 10759.
(15) Péron, N.; Mészáros, R.; Varga, I.; Gilányi, T. *J. Colloid Interface Sci.* **2007**, *313*, 389.
(16) Feitosa, E.; Brown, W.; Vasilescu, M.; Swanson-Vethamuthu, M. *Macromolecules* **1996**, *29*, 6837.
(17) Feitosa, E.; Brown, W.; Swanson-Vethamuthu, M. *Langmuir* **1996**, *12*, 5985.
(18) Feitosa, E.; Brown, W.; Hansson, P. *Macromolecules* **1996**, *29*, 2169.
(19) Gianni, P.; Barghini, A.; Bernazzani, L.; Mollica, V.; Pizzolla, P. *J. Phys. Chem. B* **2006**, *110*, 9112.
(20) Gianni, P.; Bernazzani, L.; Carosi, R.; Mollica, V. *Langmuir* **2007**, *23*, 8752.
(21) Gianni, P.; Barghini, A.; Bernazzani, L.; Mollica, V. *Langmuir* **2006**, *22*, 8001.
(22) Feitosa, E.; Brown, W.; Wang, K.; Barreleiro, P. C. A. *Macromolecules* **2002**, *35*, 201.
(23) Ge, L.; Zhang, X.; Guo, R. *Polymer* **2007**, *48*, 2681.
(24) Diab, C.; Winnik, F. M.; Tribet, C. *Langmuir* **2007**, *23*, 3025.
(25) Lad, M. D.; Ledger, V. M.; Briggs, B.; Green, R. J.; Frazier, R. A. *Langmuir* **2003**, *19*, 5098.
(26) Kalyanasundaram, K.; Thomas, J. K. *J. Am. Chem. Soc.* **1977**, *99*, 2039.
(27) Wang, X.; Wang, J.; Wang, Y.; Ye, J.; Yan, H.; Thomas, R. K. *J. Colloid Interface Sci.* **2005**, *286*, 739.
(28) Liu, Y.; Guo, R. *Biomacromolecules* **2007**, *8*, 2902.
(29) De, S.; Girigoswami, A. *J. Colloid Interface Sci.* **2004**, *271*, 485.
(30) Toerne, K.; von Wandruszka, R. *Langmuir* **2002**, *18*, 7349.
(31) Groot, R. D. *Langmuir* **2000**, *16*, 7493–7502.
(32) Borisov, O. V.; Halperin, A. *Macromolecules* **1996**, *29*, 2612.
(33) Chari, K.; Kowalczyk, J.; Lal, J. *J. Phys. Chem. B* **2004**, *108*, 2857.
(34) Qiao, L.; Easteal, A. J. *Colloid Polym. Sci.* **1998**, *276*, 313.
(35) Toboada, P.; Castro, E.; Mosquera, V. *J. Phys. Chem. B* **2005**, *109*, 23760.
(36) Li, Y.; Xu, R.; Couderc, S.; Bloor, D. M.; Holzwarth, J. F.; Wyn-Jones, E. *Langmuir* **2001**, *17*, 5742.
(37) Wolszczak, M.; Miller, J. *J. Photochem. Photobiol., A* **2002**, *147*, 45.
(38) Guo, R.; Liu, T.; Yu, W. *Langmuir* **1999**, *15*, 624.
(39) Sharma, K. S.; Hassan, P. A.; Rakshit, A. K. *Colloids Surf., A.* **2006**, *289*, 17.
(40) López-Esparza, R.; Gurdeau-Boudeville, M. A.; Cambin, Y.; Rodríguez-Beas, C.; Maldonado, A.; Urbach, W. *J. Colloid Interface Sci.* **2006**, *300*, 105.

JP910315E